JOURNAL OF AGRICULTURAL AND FOOD CHEMISTRY

Article

Structural variation and microrheological properties of a homogeneous polysaccharide from wheat germ

liyuan Yun, Tao Wu, rui Liu, kun Li, and Min Zhang

J. Agric. Food Chem., **Just Accepted Manuscript** • DOI: 10.1021/acs.jafc.7b04730 • Publication Date (Web): 19 Jan 2018

Structural variation and microrheological properties of a homogeneous polysaccharide from wheat germ

Liyuan Yun[#], Tao Wu[#], Rui Liu, Kun Li, Min Zhang[*]

State Key Laboratory of Food Nutrition and Safety (Tianjin University of Science and Technology); Key Laboratory of Food Nutrition and Safety, Ministry of Education, Tianjin 300457, China

 # These authors contributed to the work equally and should be regarded as co-first authors.

Corresponding Author: Min Zhang

Telephone: +86-22-60912430

E-mail address: zm0102@sina.com; wutaoxx@gmail.com

Abstract

A novel polysaccharide (WGP) was purified from crude wheat germ polysaccharide by Sephacryl S-500HRgel filtration. The molecular weight of WGP was determined as 4.89×10^6 Da and consisted of arabinose, xylose, glucose and galactose. Methylation analysis and 1D/2D nuclear magnetic resonance was used to analysis the structural characterization of WGP. WGP was mainly a backbone composing of (1→4)-linked-β-D-Xylp (19.01%), (1→3, 4)-linked-β-D-Xylp (26.27%) residues, which was branched of (1→5)-linked α-L-Araf (28.09%), and (1→3,6)-linked β-D-Galp (12.11%) with β-D-Glcp (14.52%) as terminal unit. The calculated values of Turbiscan stability indexes suggested that WGP (0.1–0.5 mg/mL) is a stable system. Microrheology results showed that WGP can form gel behavior when the concentration of WGP range from 0.1 to 3 mg/mL. Results of in vitro assay showed that WGP could cause the proliferation of RAW264.7 macrophages, upregulate the release of TNF-α and IL-8 in the lymphocytes.

Keywords: Wheat germ polysaccharide; structural features; microrheology; stability; immunoregulatory activity

18 **Introduction**

19 Wheat is the most significant staple diet in the world especially in Asia and has
20 been used as a major segment of different kinds food products.[1] Wheat germ is a
21 highly nutritive by-product of the wheat processing. Wheat germ provides more
22 protein,[2] minerals,[3] E-vitamins,[4] dietary fiber, and unsaturated fatty acids[5] than wheat
23 flour. The antioxidants separated from wheat germ have been applied to prevent
24 cardiovascular diseases and cancer.[6] Therefore, wheat germ serves as a proper
25 medium to transmit nutritional ingredient to human diet. However, wheat germ is
26 almost removed during milling [7, 8]and is widely applied to animal feed, which has few
27 commercial uses and causes energy waste.

28 Many researchers recently focused on wheat germ agglutinin activity,[9, 10] germ
29 oil properties[11, 12], and wheat protein structure studies,[13–15] whereas few studies
30 identified the nonstarch polysaccharides of wheat germ. Meanwhile, polysaccharides,
31 such as dietary fiber and starch, have been mixed in protein, suspensions, and
32 emulsions to enhance their stability with respect to creaming or sedimentation. Many
33 studies reported that the immunostimulatory activity of polysaccharide may be one of
34 the mechanisms underlying its antitumor, anticomplementary, and anti-inflammatory
35 functions.[16] Therefore, the physicochemical properties (stability, thermal, and
36 rheological) and bioactivity of the wheat germ polysaccharide must be characterized.
37 Accordingly, the immunostimulatory activity could be a significant biological activity
38 of polysaccharides.[16]

39 In this report, a water-soluble wheat germ polysaccharide (WGP) was first
40 separated from wheat germ and characterized for its chemical structure. Physical
41 stability of WGP was assessed by an optical analyzer (Turbiscan), diffusing wave
42 spectroscopy (DWS), and thermogravimetric analysis (TGA). The immune activity of

43 WGP was evaluated.

44 The structure, physicochemical properties, and immunostimulatory activity help
45 in characterizing wheat germ polysaccharides. In addition, the results are essential to
46 predict their far-reaching utilization in the industrial spheres.

47 **Materials and methods**

48 **Materials.** Wheat germ was provided by FADA Flour Group in Shandong, China.
49 Reagents and solvents in the study were of analytical purity (AR) grade.

50 **Sample preparation.** Wheat germ was ground by a high-speed disintegrator into
51 a powder and sieved through a 60 mesh screen. Petroleum ether was used to remove
52 the fat of WGP (1:3 g/mL) in a Soxhlet apparatus by reflowing at 60 °C for 7 h.
53 Afterward, the powder was dried at room temperature for subsequent experiments.

54 **Extraction of polysaccharides from wheat germ.** After the amylase enzymatic
55 hydrolysis, precipitates were collected via centrifugation (4000 r/min, 10 min).The
56 precipitates were extracted with hot water (1:5, w/v) for three times at 70°C and 44
57 min for each time. Solutions were concentrated with rotary evaporator (RE-52AA,
58 Shanghai, China) at 60°C under vacuum and then 95% ethanol (1:4, v/v) was used to
59 precipitate at 4°C overnight. Precipitation was obtained by centrifugation and
60 re-dissolved in distilled water. Protein was removed according to Sevage method,
61 followed by exhaustive dialysis with distilled water for 72 h. After being lyophilized,
62 solution was concentrated under reduced pressure to produce the crude polysaccharide
63 (cWGP).[17] Each cWGP sample was weighted with an analytical balance (CPA225D,
64 Beijing, China), according to the following equation to calculated the extraction yield
65 (Y) :[18]

66 $$Y\% = \frac{\text{weight of the cWGP}}{\text{weight of sample}} \times 100 \quad (1)$$

67 **Isolation and purity of WGP.** In brief, 2 mL of cWGP (40 mg/mL) was purified
68 by Sephacryl S-500 HR chromatography column (1.6 cm×45 cm). The eluents with
69 distilled water were collected in test tubes (2 mL/tube) and detected by using
70 phenol-sulfuric acid method.[19] Two fractions were gathered and the first fraction
71 (WGP) was studied in this part the second fraction was studied in the following study.
72 WGP was further purified with Sepharose 4B column by using water as an eluent.

73 High-performance liquid chromatography (HPLC) was used to analysis the
74 homogeneity and molecular weight determination of WGP. 20 μL WGP (5 mg/mL)
75 aqueous solution was subjected to a Waters LC-20AT HPLC system (Shimadzu
76 Company, Japan) with OHpak SB-805 HQ column (8.0 mm×300 mm) and equipped
77 with a refractive index detector (Shimadzu RID-10A, Kyoto, Japan). Ultrapure water
78 was used to elute at a flow rate of 0.8 mL/min. According to the calibration curve,
79 which was provided by the dextran standards (5300, 3755, 2400, 2000, 500, 110, 70,
80 40, and 10 kDa), the average molecular weight of WGP was computed.

81 **Determination of chemical composition of WGP.** The carbohydrate content
82 was analyzed by the method of phenol-sulfuric acid,[19] and xylose was used a standard.
83 The content of nitrogen was determined using Kjeldahl method and multiplied by a
84 factor of 5.45 to determine the protein content.[20] The method of carbazole-sulfuric
85 acid was used to detect the content of uronic acid, and glucuronic acid was used as a
86 standard. Orcinol-hydrochloric acid method was applied to determine the pentosan
87 content, and xylose was used as standard.[21]

88 **Measurement of monosaccharide components.** 10 mg WGP was hydrolyzed
89 by 1mL trifluoroacetic acid (TFA, 2M) at 120°C for 6 h. The hydrolyzed product was
90 dried by rotary evaporation and then added 1 mL of methanol repeatedly three times
91 to completely remove TFA. 30 mg sodium borohydride ($NaBH_4$) and 2 mL distilled

92 water was added to the hydrolyzed product, then completely reaction at room
93 temperature for 1.5 h. After that, acetic acid was used to consume the superfluous
94 $NaBH_4$. The mixture solution was concentrate to dry by rotary evaporation and added
95 2 mL 0.1% (v/v) hydrochloric acid methanol solution to the dried mixture production
96 repeatedly three times. Finally, 0.5 mL pyridine and 0.5 mL acetic anhydride was
97 added to the mixture production and reacting at 105 ^{o}C for 1 h. The acetylated
98 derivatives were produced and filtered through a 0.22 μm membrane for gas
99 chromatography (GC) analysis. [22] The GC equipped with an Agilent 7890A instrument
100 and an OV-1701 capillary column (30 m×0.32 mm×0.5 um).

101 The temperature produce was set as follows: 150°C for 1 min; 10°C /min from
102 150 to 200 °C; 200 °C for 10 min; 5 °C /min from 200 to 220 °C; 220 °C for 5 min;
103 1.5 °C /min from 220 to 240 °C; 240 °C for 20 min. Injector temperature and detector
104 temperature was 240 °C and 280 °C, respectively. The injection volume is 5 μL and
105 the split ratio is 1:10. The monosaccharides were analyzed by comparing with
106 monosaccharide standard.[23]

107 **Periodate oxidation and Smith degradation analysis.** The degree of branching
108 and provision of the residues along the polysaccharide chain was analyzed by
109 Periodate oxidation and Smith degradation. Briefly, 30 mg WGP was dissolved in 30
110 mL of sodium periodate ($NaIO_4$, 0.02 M) and maintained in the dark at 4 °C. The
111 mixture was then dialyzed for 24 h[24] and reduced with 30 mg $NaBH_4$ at 4 °C for 12 h.
112 50% acetic acid was used to neutralize and then the mixture production was dialysis
113 by water. The retentate was lyophilized and hydrolyzed by 2 M TFA at 100 °C for 3 h.
114 Product was hydrolyzed and acetylated as described in the monosaccharide
115 composition analysis section and was then subjected to GC analysis.

116 **Methylation analysis.** WGP was methylated by the reported method of

117 Hakomori with appropriate modification.[25] Briefly, 25 mg WGP was completely
118 dissolved in 2 mL of dimethyl sulfoxide and 50 mg of sodium hydroxide (NaOH)
119 powder. After that, 1 mL of methyl iodide was gradually added to the mixed solution
120 maintained in dark and sonicated for 1h. The disappearance of O-H band (3200–3700
121 cm^{-1}) in the infrared spectrum means that the accomplishment of methylation. After
122 that, methylated products were hydrolyzed, reduced, and acetylated to produce alditol
123 acetates, and analyzed by gas chromatography–mass spectrometry (GC–MS).[26]
124 According to mass spectra to identify the methylated products. By peak areas and
125 suiting response factors in GC-MS to analysis the relative molar ratios of products.[24]

126 **FT-IR analysis.** 1 mg WGP dried powder was ground with KBr powder and then
127 pressed into pellets for FT-IR measurement (Thermo Nicolet, MA, USA). The test
128 frequency is 4000 to 400 cm^{-1}.

129 **1D and 2D NMR analysis.** Dried WGP was exchanged with D_2O for several
130 times.[24] In brief, 20 mg of deuterium-exchanged polysaccharide was dissolved in 0.5
131 mL of D_2O (99.8% D, Cambridge Isotope Laboratories Inc., Andover, MA, USA) and
132 then added in a NMR tube. 1D and 2D NMR spectra were determined by an Avance
133 III 400 MHz NMR spectrometer (Bruker Corporation, Switzerland).

134 **Conformational structure analysis.** Congo red was used to analysis the
135 conformational structure of polysaccharides solution. 2 mL WGP (1 mg/mL) aqueous
136 solution was mixed with 2 mL Congo red (80 μmol/mL). The mixed solution was
137 dissolved with NaOH (0-0.5 M). The λmax of the Congo red–polysaccharide
138 solutions at different NaOH concentrations was used to evaluate the transition from a
139 triple-helical preparation to a single-stranded conformation. [27]

140 **Morphology feature analysis.** Scanning electron microscopy (SEM) and atomic
141 force microscopy (AFM) were used to measure the morphology features.

142 The SEM images of WGP (500×, 1000×, and 2000× magnifications) were
143 analyzed by a Hitachi SU-1510 system (Hitachi, Pleasanton, CA, 170 USA). Sputter
144 coater (Hummer XP, Anatech, CA, USA) was used to coat a thin layer of gold onto
145 the sample.

146 AFM has been recently used to recognize the surface atoms.[28] WGP aqueous
147 solution (0.1 μg/mL) was dropped into the surface of mica plate then dried at room
148 temperature for overnight.[29] Subsequently, the images of WGP were determined by
149 AFM (JEOL, Japan) with a tapping mode. The imaging force was approximated to be
150 0.05–3.0 nN, and the resonant frequency was 2 kHz.[30]

151 **Physicochemical property**

152 **Sample preparation.** WGP was treated with distilled water in different
153 concentrations (0.1, 0.5, 1, 3, and 5 mg/mL) with gentle stirring at room temperature
154 until dispersion.

155 **Turbiscan analysis.** Turbiscan ASG (Formulaction, Union, France) was used to
156 determine the polysaccharide solution stability.[31] The instrument is equipped with a
157 detection head, which scans the sample cell from top to bottom. The percentage of
158 backscattering[32] and transmission (T) was measured by using the height of the tube to
159 calculate the rate of polysaccharide solution destabilization.[33,34] According to scanning
160 the sample at preset intervals, the light flux backscattering and macroscopic
161 fingerprint of sample was acquired. Thus, the stability of polysaccharide solution was
162 determined by Turbiscan stability index (*TSI*).[35]

163 In this part, *TSI* was measured by a special computer program Turbiscan Easy
164 Soft. The formula as follow:

165 $$TSI = \sum_{i} \frac{\sum_{h} \left| scan_{i}(h) - scan_{i-1}(h) \right|}{H} \quad (2)$$

166 $scan_i(h)$, the average backscattering for i time; $scan_{i-1}(h)$, the average backscattering
167 for i−1 time; H, the height of sample. Clearly, *TSI* considers all individual scans in an
168 assay. The value of sample is calculated from the averaging. Low *TSI* indicates a
169 steady system.[36]

170 **Microrheological behavior.** 20 mL WGP aqueous solution with different
171 concentrations (0.1, 0.5, 1, 3, and 5 mg/mL) was added to sample cells and maintained
172 at 27 °C (±0.1 °C). The results were measured by Rheolaser Master (Formulaction,
173 l'Union, France).

174 **Thermogravimetric analysis.** The TA Instrument (model TGA Q50) was used
175 for the thermogravimetric analysis. 3–5 mg WGP was performed on a dried aluminum
176 crucible under nitrogen. The preset temperature was 30°C to 800°C and the heating
177 rate was10 °C/min. Manometric pressure was remained at 101 kPa.[29]

178 Differential scanning calorimetry (DSC) was equipped with a TA-60WS
179 Collection Monitor DSC system (Shimadzu). In brief, 2 mg of WGP was placed in
180 aluminum pans. The test temperature was 30 °C to 200 °C, and the heating rate was
181 10 °C/min. Denaturation peak temperature (Tp) was analyzed by DSC thermograms.

182 **Assay of immunomodulatory activity of WGP**

183 **The determined of cell proliferation ability**. According to MTT assay[16], the
184 influence of polysaccharides on proliferation of RAW264.7 cells was analyzed. In
185 brief, 100 μL/well RAW264.7 cell suspension (1×10^6 cells/mL) was incubated in
186 96-well plate (37 °C, 5% CO_2) for 12 h. The adherent RAW264.7 cells were incubated
187 with a medium containing various concentrations of WGP (10, 20, 40, 60, and 80.0
188 μg/mL) and complete medium alone (blank control) or lipopolysaccharide (LPS) (5.0

189 μg/mL, positive control) for 48 h. After adding 150 μL of dimethyl sulfoxide solution,
190 the absorbance was determined by microplate reader at 540 nm.[38]

191 **Real-time reverse transcription polymerase chain reaction (PCR)**. The
192 immunocompetence of WGP in activating RAW264.7 cells was analyzed by
193 monitoring its effects on the release of tumor necrosis factor (TNF)-α and interleukin
194 (IL)-8. Total RNA from WGP-treated, untreated and LPS-treated RAW264.7 cells
195 were extracted with Trizol reagent (Gibco-BRL) following the manufacturer's
196 protocol.[38] RAW264.7 cells (1×10^6/mL) adhered to the six-well plate with WGP (40
197 μg/mL) for 48 h. The qPCR was prepared by a 25 μL reaction volume, which
198 contained 12.5 μL SYBR Mix, 1 μL cDNA templates, 1 μL of each forward and
199 reverse primer, and 9.5 μL PCR grade sterile water. The results were shown as the
200 ratio of optimal density to GAPDH, which was used as an internal reference. The
201 primers were designed as follows: GAPDH (forward: TGGCCTTCCGTGTTCCTAC,
202 reverse:GAGTTGCTGTTGAAGTCGCA);TNFα(forward:AGGAGGAGTCTGCGA
203 AGAAGA,reverse:GGCAGTGGACCATCTAACTCG);IL-8(forward:TCGAGACCA
204 TTTACTGCAACA，reverse: CATTGCCGGTGGAAATTCCTT).

205 **Statistical analysis.** The results are represented by mean±standard deviation
206 and estimated using one-way ANOVA, followed by Student's t-test. Each result was
207 performed in triplicate. $p<0.05$ and $p<0.01$ were statistically significant.

208 **Results and discussion**

209 **Composition analysis of WGP.** Crude polysaccharides were isolated from the
210 defatted wheat germ with a yield of 1.16%. cWGP was purified by Sephacryl S-500
211 HR, and two parts were collected (Figure 1A). The first-part cWGP was further
212 purified by a Sepharose 4B gel-permeation chromatography column (Figure 1B).
213 After dialysis and lyophilization of the first fraction, WGP was obtained (6.47% yield

214 from the crude extracts). In Figure 1D, a single peak was observed. The low
215 polydispersity index (Mw/Mn=1.06) revealed that the polysaccharide is a relative
216 homogeneous fraction. The average molecular weight of WGP was 4.89×10^6 Da as
217 calculated by the dextran standard curves. The neutral polysaccharide (WGP) has a
218 high molecular weight. Meanwhile, high molecular weights of water-soluble and
219 water-insoluble arabinoxylans from wheat,[39] barley, sorghum, and rye have been
220 extracted.

221 The contents of total sugar, protein, uronic acid and pentosan of WGP are shown
222 in Table 1. Figure 1C shows that WGP has weak absorption in wavelength 250–300
223 nm, possibly because of its protein or nucleic acid content. Results of UV analysis
224 agreed with the protein contents of WGP.

225 **Monosaccharide composition analysis.** WGP is mainly comprised of arabinose
226 and xylose with some glucose and galactose. Table 1 shows the ratio of arabinose,
227 xylose, galactose, and glucose. The galactose might come from arabinogalactans or
228 galctoarabinoxylans, which were found among the members of Graminae family.[40]
229 The minimal glucose content of WGP is probably attributed to β-glucan and
230 unhydrolyzed starch. The ratio of arabinose to xylose (A/X) is 0.69. The ratio is
231 different among other wheat studies[40] possibly due to the differences in wheat
232 varieties and polysaccharide extracted methods.

233 **Periodate oxidization and Smith degradation analysis.** Upon oxidation with
234 periodate, 30 mg of WGP consumed 72.70 μmol periodate and produced 21.71 μmol
235 formic acid. The consumption of periodate was more than twice that of the production
236 of formic acid, showing that one or more of (1→6), (1→2) or (1→4)-linked
237 glycosidic bonds might exist. After Smith degradation, glycerol, xylose, and galactose
238 were found (Figure 2A). Glycerol associated with the presence of (1→2) or

239 (1→6)-linked glycosidic bonds, and it also may originate from the side chains of
240 arabinose.[41] The existence of monosaccharides mean (1→3)-linked glycosidic bonds
241 exist in WGP. Several precise glycosidic bonds were confirmed in the methylation
242 analysis.[42]

243 **Methylation analysis of WGP.** Glucosidic bond types of natural
244 polysaccharides were determined by the method of methylation. Results of
245 methylation analysis are shown in Table 2. According to the CCRC Spectral Database
246 for PMAAs, the peaks were confirmed as 2,4-Me_2-Galp, 2,3,4,6-Me_4-Glcp,
247 2,3-Me_2-Araf, 2,3,-Me_2-Xylp, and 2-Me-Xylp with a molar ratio of
248 12.11%:14.53%:28.09%:19.01%:26.27%. The inference also agreed with the result of
249 Periodate oxidation and Smith degradation. Result also showed xylose residues in the
250 main chain with 1–4 linkages. Xylan backbone was mainly substituted at the O-3
251 position by arabinofuranosyl residues due to the existence of high amounts of
252 2-Me-Xylp in WGP. The unsubstituted, monosubstituted, and doubly substituted
253 xylose residues had also been studied in rice, wheat, and sorghum.[43] The results
254 showed that two forms (unsubstituted and monosubstituted) of xylose residues are
255 exist in WGP.

256 **NMR.** The 1D and 2D NMR spectra were used to analysis the structure of WGP.
257 In the proton spectrum of mono-, oligo-, and polysaccharides, all chemical shifts
258 come out in the range of 1–6 ppm. The region of 5–6 ppm is associated with
259 α-anomeric protons, and the region of 4–5 ppm is assigned to β-anomeric protons.
260 The chemical shifts variation from δ 3.4 ppm to 4.0 ppm were considered as the
261 signals correlated with the protons exist on C2–C6.[44] Thus, according to the ^{1}H
262 spectrum of WGP (Figure 3A), the resonances at 5.24 ppm was definitely due to
263 α-L-arabinose residues.[45] In addition, the signal in the anomeric region of 5.00 and

264 4.52 ppm was related to the protons of β-D-Xylp residues. Resonances at 4.4 ppm and
265 4.5 ppm were correlated with the anomeric protons of β-D-Galp residues[46] and
266 β-D-Glcp residues, respectively.

267 In COSY spectrum, an anomeric proton is a reasonable starting point of
268 assigning because it is linked to a carbon holding two oxygen atoms, presumably the
269 most downfield ^{1}H signal. As demonstrated in the COSY spectrum of WGP (Figure
270 3C), the H1–2, H2–3, H3–4, H4–5, and H5-6 correlations of WGP were observed.[47]

271 As shown in 13C NMR spectrum (Figure 3B), the signals ranging from δ 90
272 to110 ppm are related to anomeric carbons, whereas the chemical shift in δ 60–85
273 ppm is linked to non-anomeric carbons. The existence of C-1 signals (δ100–108 ppm)
274 showed that four sugar residues were all in pyran ring.[48] Some research had report that
275 C-1 signals around 107–109 ppm is furan ring.[48] The signals at approximately 108.4–
276 109.2 ppm are attributed to anomeric carbon atoms of α-linked arabinofuranos.[49]
277 Peaks are associated with the anomeric carbon of arabinose residues due to the
278 diversity-linked arabinosyl residues, showing slight variations in the mode of
279 linkage.[40]

280 Five pairs of ^{1}H and ^{13}C signals of anomeric CH were caused by five different
281 forms of glycosidic bonds. According to chemical shifts and the relevant HMQC
282 correlations, these bonds were assigned at δ 4.45/102.71, 4.53/103.35, 5.24/109.16,
283 4.65/104.18, and 5.00/107.69 ppm (Figure 3D). The result showed that five types of
284 glycosidic bonds existed in WGP. From the HMQC correlations, residue A was
285 identified as a galactose residue. The else signals of residue A were determined as
286 δ73.40/3.69 (CH–2), 74.29/4.09 (CH–3), 73.72/3.57 (CH–4), 76.56/4.01 (CH–5), and
287 62.93/3.62 (CH–6). Meanwhile, the chemistry shifts of other residues was identified,
288 the results were shown in Table 3.

289 According to the heteronuclear multiple bond correlation (HMBC) spectrum
290 (Figure 3E) of WGP, five residues were associated with each other were identified.
291 The correlations of each sugar residues in HMBC spectrum are identified as follows:
292 E H-1 (δ 5.08) and E C-4 (δ 83.40), C H-1 (δ 5.24) and E C-3 (δ 84.13), A H-3 (δ 4.05)
293 and C C-5 (δ 61.20), and B C-1 (δ 103.35) and A H-6 (δ 3.57). In HMBC spectrum,
294 the peaks at δ 5.08/83.40 and δ 5.24/84.13 were observed. Residues E and E were
295 correlated as E-(4→1)-E due to the signal at δ5.08 connected with H-1 in residue E, δ
296 83.40 to C-4 in residue E. Residues C and E were associated as E-(3→1)-C due to the
297 signal at δ5.24 corresponded to H-1 in residue C, and the signal at δ84.13
298 corresponded to C-3 in residue E. In addition, the cross-peaks at δ 4.05/61.20 was
299 identified to the inter-residue A H-3, C C-5, which showed the residues A and C were
300 associated as A-(3→5)-C. The chemistry shift at δ3.57/103.35 were identified to the
301 inter-residue A H-6, B C-1, which showed residues A and B were combined as B-(6→
302 1)-A. Thus, in Figure 4, the structure of WGP was defined as a backbone made up of
303 (1→4)-linked β-D-xylose. The substitute at O-3 of β-D-xylose composed of
304 (1→5)-linked α-L-arabinose and (1→3,6)-linked β-D-galactose, the β-D-glucose as
305 terminal unit.

306 **FT-IR spectra.** According to the FT-IR spectrum (Figure 2B) the different
307 absorption bands were identified.[50] The broad peak appeared at 3405.11 cm^{-1} was
308 produced by O–H stretching vibrations of hydroxyl groups of polysaccharide fractions.
309 The weak peak at 2925.7 cm^{-1} was caused by C–H stretching vibration. The peak at
310 1639.92 cm^{-1} was mainly connected with absorbed water due to the hemicelluloses is
311 easily combined with water. Nevertheless, the macromolecules in solid state were
312 easily hydrated due to the disordered structures.[51] Peaks at 1400–1200 cm^{-1} was on
313 behalf of the C–H deformation vibration. This signal showed variations in intensity

314 with a decrease and displacement at 1039.54 in the WGP that is typical of the β-(1-3)
315 xylans.[52] In the report of Yang et al.,[53] β-D-glucopyranose and β-D-galactose had
316 absorptive peaks at 905–876 and 876–886 cm^{-1}, respectively. The peak at 897.72 cm^{-1}
317 ascribed to the C-1 group frequency or ring frequency, this was also a typical of
318 β-glycosidic linkages.[54] Band at 817.39 cm^{-1} was the characteristic of α-glycosidic
319 linkages. The relative strength of the peak at 817.39 cm^{-1} was considerably lower than
320 that of the 897.72 cm^{-1} peak, indicating that the linkages of WGP was mainly
321 β-glycosidic with the amount of α-glycosidic bonds.

322 **Conformational structure of WGP.** Congo red method was applied at different
323 concentrations of NaOH (0.05–0.5 M) solution to identify the triple helix
324 conformation of WGP. As shown in Figure 2C, an obvious shift of maximum
325 absorption wavelength from 500 nm to 520 nm was induced by the presence of the
326 polysaccharides in Congo red solution, indicating that polysaccharide–Congo red
327 compound had formed. With the increase of concentrations of NaOH, the maximum
328 absorption wavelength decreased slightly. With the increase of concentrations of
329 NaOH, the triple-helix conformation will translate into single coil conformation, and
330 the maximum absorption wavelength will decrease dramatically. Thus, the result
331 indicated that WGP did not exhibit a triple helical conformation.[55]

332 **Morphological characteristics analysis.** Figure 5A shows the surface
333 morphology of WGP determined by SEM. The surface topography of WGP showed a
334 reticular layer with spherical particles or oval granules. The surface morphology may
335 provide an opportunity to connect linkages between polymers.[2]

336 Figure 5B shows the surface morphology of WGP determined by AFM. Many
337 different spherical sizes existed in the images. The result indicated that the molecular
338 aggregation has occurred, and polysaccharide molecules have different sizes of

339 spherical structure. The height of 1.73 nm showed that WGP was not a single sugar
340 chain molecule but a group of molecules. The hydrogen bonds in polysaccharides can
341 provide the inter- and intramolecular interactions with each other or with water
342 molecule, which induces a significant effects on molecular aggregation.[56] These
343 effects entangle the polysaccharide molecules and form the collective structure.

344 **Physicochemical property.** The viscosity of polysaccharide solution was
345 correlated with its conformation and molecular weight.[57] Therefore in this work, the
346 physicochemical properties of WGP had been studied.

347 **Physical stability analyzed by Turbiscan.** According to the backscattering
348 technology, Turbiscan was used to evaluate the effects of WGP on stability. In Figure
349 6 and Table 4, the stability index of WGP increased from 0.4 to 23.14. When the
350 concentrations increased from 3 mg/mL to 5 mg/mL, *TSI* exhibited a remarkable
351 increase. This phenomenon occurred because with the increasing of concentration, the
352 molecular structure may form settling or molecular crystal and cause the aggregation
353 of polysaccharide solution.[34]

354 **Microrheological analysis.** Microrheology is commonly used to analyze and
355 trace the motion of droplets and the interactions. MSD of droplets in different
356 concentrations was analyzed as a function of time.[41]

357 Figure S1 in the supplementary materials shows MSD curves of WGP at
358 different aging times. The MSD curves move from long to short displacement
359 signifying an increase in elasticity. The MSD curves move from short to long
360 decorrelation time signifying an increase in the viscosity. The MSD curve showed that,
361 as the aging time prolongs, the elasticity of WGP increased and then decreased. At the
362 beginning, the elasticity increased may be due to polysaccharide and water combined
363 gradually and then achieved a steady state.[6] The major advantage of this approach is

364 that the diffusive motions of many droplets can be recorded simultaneously while
365 retaining the information for each of the individual droplets trajectories.[58] The
366 intensity correlation function can be immediately converted into a time-dependent
367 MSD,[34] which is a immediate and non-invasive probe of medium properties.[33]

368 Elasticity index (*EI*) value indicates the elasticity strength of polysaccharide
369 solution.[34] *EI* of WGP is shown in Table 4. *EI* of WGP increased first and then
370 decreased with increasing concentration (0.5–5 mg/mL). This phenomenon occurred
371 because when the concentration increases, the probability of precipitation also
372 increases.

373 Macroscopic viscosity index (*MVI*) value stands for the macroscopic viscosity
374 without shear[34] and is associated with the inversed MSD slope in linear scale and
375 connected with the macroscopic viscosity.[59] In Table 4, when the concentration is 0.1
376 mg/mL, *MVI* reaches to 5.78 Pa s, possibly because the molecular activity is relatively
377 easy in a low concentration, which can easily afford several spaces for the motion of
378 the chain segments[60] and the wide Brownian motion.

379 When the concentration ranges from 0.5 mg/mL to 3 mg/mL, *MVI* of WGP
380 increases as the concentration increases. However, when the concentration reached to
381 5 mg/mL, the macroscopic viscosity decreased significantly. These results suggested
382 that as the concentration increases, the molecular chain gradually expands in the
383 system. A high degree of polymerization was highly viscous in aqueous solution[61], but
384 when the concentration is too high (5 mg/mL), the movement of the molecules is
385 limited, resulting in separation and aggregation.

386 The solid–liquid balance (*SLB*) connecting with MSD slope at short
387 decorrelation time: a key value of deformation from liquid domination to solid
388 domination is SLB=0.5. The $0.5<SLB<1$ stand for liquid behavior dominates, whereas

389 0<*SLB*<0.5 indicates a gel behavior and solid behavior dominates.[59] In Table 4, as the
390 concentration of WGP ranging from 0.1 mg/mL to 3 mg/mL, *SLB*s are smaller than
391 0.5. The result indicated that solid dominate the dispersions and form gel behavior.
392 When concentration is greater than 3 mg/mL, *SLB* of WGP is greater than 0.5 and less
393 than 1. This finding may be due to high concentration of polysaccharides (more than 3
394 mg/mL), resulting in flocculation and precipitation giving rise to an instability system.

395 **Thermal analysis.** Weight loss and degradation temperature are shown in Table
396 5. The thermal degradation curves and their first derivatives are shown in Figure 7A.
397 Initial weight loss in the temperature range from 30 °C to 150 °C for WGP is ascribed
398 to the loss of free and bound water. Temperature range of 200 °C–400 °C was due to
399 the decomposition of polysaccharides.[2]

400 The DSC thermograms of WGP are presented in Figure 7B. The DSC curve of
401 WGP pointed an obvious endothermic peak at 82.57 °C, which might be due to the
402 dehydration or the loss of peripheral polysaccharide chains and dehydroxylation
403 reactions.[62]

404 **Immunomodulatory activity in vitro of WGP**

405 **Effects of WGP on the proliferation of macrophages.** As shown in Figure 8A,
406 WGP significantly increased the viability of RAW264.7 cells from 10 μg/mL to 80.0
407 μg/mL. Compared with blank control, WGP can observably stimulated the viability of
408 RAW264.7 cells ($p<0.01$). When the concentration of WGP is 40 μg/mL, the
409 proliferation index reaches to 92.136%±0.899%.

410 **Effects of WGP on production of cytokines**. As shown in Figure 8B, after the
411 treatment of WGP, the levels of TNF-α and IL-8 cytokines increased. This result
412 showed that WGP significantly increased the secretion of TNF-α and IL-8 in
413 RAW264.7 cells when stimulated for 48 h. The results further confirmed that WGP

414 could promote the function of macrophages.

415 Accoridng to methylation, GC–MS, FT-IR, and 1D/2D NMR, the linkages of
416 WGP were 1,4-linked β-D-Xylp (19.01%), 1,3,4-linked β-D-Xylp (26.27%),
417 1,5-linked α-L-Araf (28.09%), 1,3,6-linked β-D-Galp (12.11%), and T-linked Glcp
418 (14.52%). Physicochemical properties analysis results showed that the gel behavior
419 dominates the dispersions of WGP (0.1–3 mg/mL) and probably interacted with the
420 molecular weight, the link location of glycoside residues, and the link order of
421 glycoside. In vitro, WGP has a potent immunostimulating activity possibly due to
422 its monosaccharide composition, sugar residues, and physicochemical properties.[63]
423 Future studies should focused on the possible mechanisms of immunomodulatory
424 action of WGP in in vivo assay. The study of structure, physicochemical properties,
425 and immunostimulating activity of wheat germ polysaccharides will enrich and
426 expand the application of wheat germ polysaccharide.

427 **Associated content**

428 **Supporting Information**

429 **Figure S1** The Mean Square Displacement vs time curves for WGP
430 (polysaccharide from wheat germ) (the first curves are in blue, then green, and lastly
431 in red; A, B, C, D, E was the concentration of WGP at 0.1, 0.5, 1, 3, 5 mg/mL
432 respectively).

433 **Abbreviation**

434 WGP, wheat germ polysaccharide; HPLC, high performance liquid chromatography;
435 FT-IR, fourier-transform infrared spectroscopy; NMR, nuclear magnetic resonance.

436 **Acknowledgements**

437 This work was supported by the Special Fund for Agroscientific Research in the
438 Public Interest [201303071]; Innovation of modern Agricultural Project [F17RO2];

Fundamental Research Funds for the Tianjin Universities [2017KDZD02]; National Natural Science Foundation of China [31501475]; Tianjin Science and Technology Commission [15JCQNJC46300]; and the Ph.D. Training Foundation of the Tianjin University of Science and Technology [2016002].

Conflict of interest statements

The authors state no competitive financial interest

445 **References**

446 1. Hamada, H.; Linghu, Q.; Nagira, Y.; Miki, R.; Taoka, N.; Imai, R., An in planta
447 biolistic method for stable wheat transformation. Sci. Rep. **2017**, 7.
448 2. Zhang, L.; Zuo, B.; Wu, P.; Wang, Y.; Gao, W., Ultrasound effects on the
449 acetylation of dioscorea starch isolated from Dioscorea zingiberensis C.H. Wright.
450 Chemical Engineering & Processing Process Intensification. **2012**, 54, 29-36.
451 3. Brandolini, A.; Hidalgo, A., Wheat germ: not only a by-product. Int. J. Food Sci.
452 Nutr. **2012**, 63 Suppl 1, 71.
453 4. Leenhardt, F.; Fardet, A.; Lyan, B.; Gueux, E.; Rock, E.; Mazur, A.; Chanliaud, E.;
454 Demigné, C.; Rémésy, C., Wheat germ supplementation of a low vitamin E diet in rats
455 affords effective antioxidant protection in tissues. J. Am. Coll. Nutr. **2008**, 27,
456 222-228.
457 5. Olah, N.; Vlase, L.; Marculescu, A., The study of fatty acids from different sea
458 buckthorn and wheat germ extracts. Revista de Chimie -Bucharest- Original Edition.
459 **2007**, 58, 365-367.
460 6. PéRezjiméNez, J.; Arranz, S.; Tabernero, M.; DíAzrubio, M. E.; Serrano, J.; Goni,
461 I.; Sauracalixto, F., Updated methodology to determine antioxidant capacity in plant
462 foods, oils and beverages: Extraction, measurement and expression of results. Food
463 Research International. **2008**, 41, 274-285.
464 7. Sun, R.; Zhang, Z.; Hu, X.; Xing, Q.; Zhuo, W., Effect of wheat germ flour
465 addition on wheat flour, dough and Chinese steamed bread properties. Journal of
466 Cereal Science. **2015**, 64, 153-158.
467 8. Marti, A.; Torri, L.; Casiraghi, M. C.; Franzetti, L.; Limbo, S.; Morandin, F.;
468 Quaglia, L.; Pagani, M. A., Wheat germ stabilization by heat-treatment or sourdough
469 fermentation: Effects on dough rheology and bread properties. LWT - Food Science

470 and Technology. **2014**, 59, 1100-1106.

471 9. Kaur, K.; Sodhi, R. K.; Katyal, A.; Aneja, R.; Jain, U. K.; Katare, O. P.; Madan, J.,
472 Wheat germ agglutinin anchored chitosan microspheres of reduced brominated
473 derivative of noscapine ameliorated acute inflammation in experimental colitis.
474 Colloids & Surfaces B Biointerfaces. **2015**, 132, 225-235.

475 10. Kim, Y. S.; Kong, W. H.; Kim, H.; Hahn, S. K., Targeted systemic mesenchymal
476 stem cell delivery using hyaluronate - wheat germ agglutinin conjugate. Biomaterials.
477 **2016**, 106, 217-227.

478 11. Gumus, Z. P.; Guler, E.; Demir, B.; Barlas, F. B.; Yavuz, M.; Colpankan, D.;
479 Senisik, A. M.; Teksoz, S.; Unak, P.; Coskunol, H., Herbal infusions of black seed and
480 wheat germ oil: Their chemical profiles, in vitro bio-investigations and effective
481 formulations as Phyto-Nanoemulsions. Colloids & Surfaces B Biointerfaces. **2015**,
482 133, 73-80.

483 12. Chang, C. L.; Haas, E.; Mina, A. M. M.; Bustamante, J. A.; Schneider, D.;
484 Mitchel, E.; Freilich, M.; Stanley, D., Dietary wheat germ oil and age influences fatty
485 acid compositions in adult oriental fruit flies. Journal of Asia-Pacific Entomology.
486 **2013**, 16, 285-292.

487 13. Wang, L.; Ding, Y.; Zhang, X.; Li, Y.; Wang, R.; Luo, X.; Li, Y.; Li, J.; Chen, Z.,
488 Isolation of a novel calcium-binding peptide from wheat germ protein hydrolysates
489 and the prediction for its mechanism of combination. Food Chem. **2017**.239,
490 416-426.

491 14. Wu, W.; Sun, C.; Wang, G.; Pan, Q.; Lai, F.; Li, X.; Tang, Y.; Wu, H.,
492 Immunomodulatory activities of non-prolamin proteins in wheat germ and gluten.
493 Journal of Cereal Science. **2017**, 76, 206–214.

494 15. Caporaso, N.; Whitworth, M. B.; Fisk, I. D., Protein content prediction in single

495 wheat kernels using hyperspectral imaging. Food Chem.**2017**, 240, 32-42.

496 16. Yuan, Q.; Zhao, L.; Cha, Q.; Sun, Y.; Ye, H.; Zeng, X., Structural Characterization
497 and Immunostimulatory Activity of a Homogeneous Polysaccharide from
498 Sinonovacula constricta. J. Agric. Food Chem. **2015**, 63, 7986-94.

499 17. Song, G.; Wang, K.; Zhang, H.; Sun, H.; Wu, B.; Ju, X., Structural
500 characterization and immunomodulatory activity of a novel polysaccharide from
501 Pteridium aquilinum. Int. J. Biol. Macromol. **2017**, 102, 599-604.

502 18. Tan, L.-H.; Zhang, D.; Yu, B.; Zhao, S.-P.; Wang, J.-W.; Yao, L.; Cao, W.-G.,
503 Antioxidant activity and optimization of extraction of polysaccharide from the roots
504 of Dipsacus asperoides. International Journal of Biological Macromolecules. **2015**, 81,
505 332-339.

506 19. Nwokocha, L. M.; Williams, P. A., Isolation and characterization of a novel
507 polysaccharide from seeds of Peltophorum pterocarpum. Food Hydrocolloids. **2014**,
508 41, 319-324.

509 20. Chen, Y. F.; Zhu, Q.; Wu, S., Preparation of oligosaccharides from Chinese yam
510 and their antioxidant activity. Food Chem. **2015**, 173, 1107.

511 21. Garófalo, L.; Vazquez, D.; Ferreira, F.; Soule, S., Wheat flour non-starch
512 polysaccharides and their effect on dough rheological properties. Industrial Crops and
513 Products. **2011**, 34, 1327-1331.

514 22. Zhu, J.; Liu, W.; Yu, J.; Zou, S.; Wang, J.; Yao, W.; Gao, X., Characterization and
515 hypoglycemic effect of a polysaccharide extracted from the fruit of Lycium barbarum
516 L. Carbohydrate Polymers. **2013**, 98, 8-16.

517 23. Q, Liu R, Wu T, et al. Soluble Dietary Fiber Fractions in Wheat Bran and Their
518 Interactions with Wheat Gluten Have Impacts on Dough Properties. J. Agric. Food
519 Chem., **2016**, 64:8735-8744.

520 24. Jing, Y.; Zhu, J.; Liu, T.; Bi, S.; Hu, X.; Chen, Z.; Song, L.; Lv, W.; Yu, R.,
521 Structural characterization and biological activities of a novel polysaccharide from
522 cultured Cordyceps militaris and its sulfated derivative. J. Agric. Food Chem. **2015**,
523 63, 3464.
524 25. Hakomori, S., A Rapid Permethylation of Glycolipid, and Polysaccharide
525 Catalyzed by Methylsulfinyl Carbanion in Dimethyl Sulfoxide. J. Biochem. **1964**, 55,
526 205.
527 26. Sassaki; Iacomini, G. L.; MarcelloGorin; Philip, A. J., Methylation-GC-MS
528 analysis of arabinofuranose- and galactofuranose-containing structures: rapid
529 synthesis of partially O-methylated alditol acetate standards. Anais Da Academia
530 Brasileira De Ciências. **2005**, 77, 223-234.
531 27. Lee, H. H.; Lee, J. S.; Cho, J. Y.; Kim, Y. E.; Hong, E. K., Structural
532 characteristics of immunostimulating polysaccharides from lentinus edodes. Journal
533 of Microbiology & Biotechnology. **2009**, 19, 455-461.
534 28. Sugimoto, Y.; Pou, P.; Abe, M.; Jelinek, P.; Pérez, R.; Morita, S.; Custance, Ó.,
535 Chemical identification of individual surface atoms by atomic force microscopy.
536 Nature. **2007**, 446, 64-7.
537 29. Soobhany, N.; Gunasee, S.; Rago, Y. P.; Joyram, H.; Raghoo, P.; Mohee, R.; Garg,
538 V. K., Spectroscopic, thermogravimetric and structural characterization analyses for
539 comparing Municipal Solid Waste composts and vermicomposts stability and maturity.
540 Bioresource Technology. **2017**, 236, 11.
541 30. Zhang, M.; Tang, X.; Wang, F.; Zhang, Q.; Zhang, Z., Characterization of Lycium
542 barbarum polysaccharide and its effect on human hepatoma cells. International
543 Journal of Biological Macromolecules. **2013**, 61, 270-5.
544 31. Yang, D.; Wang, X. Y.; Gan, L. J.; Zhang, H.; Shin, J. A.; Lee, K. T.; Hong, S. T.,

545 Effects of flavonoid glycosides obtained from a Ginkgo biloba extract fraction on the
546 physical and oxidative stabilities of oil-in-water emulsions prepared from a stripped
547 structured lipid with a low omega-6 to omega-3 ratio. Food Chem. **2015**, 174,
548 124-131.
549 32. Jakobsen, T. S.; Si, J. Q., The effects of xylanases in baking and characterization
550 of their modes of action. Wheat Structure.**1995**, 343-349.
551 33. Sun, C.; Wu, T.; Liu, R.; Liang, B.; Tian, Z.; Zhang, E.; Zhang, M., Effects of
552 superfine grinding and microparticulation on the surface hydrophobicity of whey
553 protein concentrate and its relation toemulsions stability. Food Hydrocolloids. **2015**,
554 51, 512-518.
555 34. Xu, D.; Zhang, J.; Cao, Y.; Wang, J.; Xiao, J., Influence of microcrystalline
556 cellulose on the microrheological property and freeze-thaw stability of soybean
557 protein hydrolysate stabilized curcumin emulsion. LWT - Food Science and
558 Technology. **2016**, 66, 590-597.
559 35. Bru, P., Particle Size and Rapid Stability Analyses of Concentrated Dispersions:
560 Use of Multiple Light Scattering Technique. Acs Symposium. **2004**, 45-60.
561 36. Shao, P.; Ma, H.; Zhu, J.; Qiu, Q., Impact of ionic strength on physicochemical
562 stability of o/w emulsions stabilized by Ulva fasciata polysaccharide. Food
563 Hydrocolloids. **2017**, 69, 202-209.
564 37. Alexander, M.; Dalgleish, D. G., Diffusing Wave Spectroscopy of aggregating
565 and gelling systems. Current Opinion in Colloid & Interface Science. **2007**, 12,
566 179-186.
567 38. Lee, J. S.; Kwon, J. S.; Yun, J. S.; Pahk, J. W.; Shin, W. C.; Lee, S. Y.; Hong, E.
568 K., Structural characterization of immunostimulating polysaccharide from cultured
569 mycelia of Cordyceps militaris. Carbohydr. Polym. **2010**, 80, 1011-1017.

570 39. Gruppen, H.; Fjm, K.; Agj, V., Water-unextractable cell wall material from wheat
571 flour. 3. A structural model for arabinoxylans. **1993**, 18, 111-128.
572 40. Revanappa, S. B.; Nandini, C. D.; Salimath, P. V., Structural variations of
573 arabinoxylans extracted from different wheat (Triticum aestivum) cultivars in
574 relation to chapati -quality. Food Hydrocolloids. **2015**, 43, 736-742.
575 41. Rao, R. S. P.; Muralikrishna, G., Structural characteristics of water-soluble
576 feruloyl arabinoxylans from rice (Oryza sativa) and ragi (finger millet, Eleusine
577 coracana): Variations upon malting. Food Chemistry. **2007**, 104, 1160-1170.
578 42. Zhang, M.; Wang, G.; Lai, F.; Hui, W., Structural Characterization and
579 Immunomodulatory Activity of a Novel Polysaccharide from Lepidium meyenii. J
580 Agric Food Chem. **2016**, 64, 1921-1931.
581 43. Nandini, C. D.; Salimath, P. V., Structural features of arabinoxylans from
582 sorghum having good roti-making quality. Food Chemistry. **2001**, 74, 417-422.
583 44. Wang, L.; Liu, F.; Wang, A.; Yu, Z.; Xu, Y.; Yang, Y., Purification,
584 characterization and bioactivity determination of a novel polysaccharide from
585 pumpkin (Cucurbita moschata) seeds. Food Hydrocolloids. **2016**, 66.
586 45. Zhang, M.; Wang, G.; Lai, F.; Wu, H., Structural Characterization and
587 Immunomodulatory Activity of a Novel Polysaccharide from Lepidium meyenii. J.
588 Agric. Food Chem. **2016**, 64, 1921.
589 46. Sun, Y.; Liu, J., Structural characterization of a water-soluble polysaccharide
590 from the Roots of Codonopsis pilosula and its immunity activity. Int. J. Biol.
591 Macromol. **2008**, 43, 279-282.
592 47. Farhadi, N., Structural elucidation of a water-soluble polysaccharide isolated
593 from Balangu shirazi (Lallemantia royleana) seeds. Food Hydrocolloids. **2017**, 72,
594 263-270.

595 48. Wang, Y.; Yin, H. P.; Lv, X. B.; Wang, Y. F.; Gao, H. Y.; Wang, M., Protection of
596 chronic renal failure by a polysaccharide from Cordyceps sinensis. Fitoterapia. **2010**,
597 81, 397.
598 49. Bradbury, J. H.; Jenkins, G. A., Determination of the structures of trisaccharides
599 by 13 C-n.m.r. spectroscopy. Carbohydrate Research. **1984**, 126, 125-56.
600 50. Zheng, R.; Jie, S.; Dai, H.; Wu, M., Characterization and immunomodulating
601 activities of polysaccharide from Lentinus edodes. International
602 Immunopharmacology. **2005**, 5, 811-820.
603 51. Kacurakova, M.; Belton, P. S.; Wilson, R. H.; Hirsch, J.; Ebringerova, A.,
604 Hydration properties of xylan-type structures: an FTIR study of xylooligosaccharides.
605 Journal of the Science of Food & Agriculture. **1998**, 77, 38–44.
606 52. Osman, N. B.; Mcdonald, A. G.; Laborie, M. P. G., Characterization of
607 water-soluble extracts from hot-pressed poplar. European Journal of Wood and Wood
608 Products. **2013**, 71, 343-351.
609 53. Yang, W.; Ying, W.; Li, X.; Ping, Y., Purification and structural characterization
610 of Chinese yam polysaccharide and its activities. Carbohydr. Polym. 2015, 117, 1021.
611 54. Gupta, S.; Madan, R. N.; Bansal, M. C., Chemical composition of Pinus caribaea
612 hemicellulose. Tappi Journal. **1987**, 38, 88-90.
613 55. Qin, C.; Huang, K.; Xu, H., Isolation and characterization of a novel
614 polysaccharide from the mucus of the loach, Misgurnus anguillicaudatus. Carbohydr.
615 Polym. **2002**, 49, 367-371.
616 56. Lingshan, K.; Ling, Y.; Tao, F.; Xiujun, Y.; Tianjing, L.; Lei, D., Physicochemical
617 characterization of the polysaccharide from Bletilla striata: effect of drying method.
618 Carbohydr. Polym. **2015**, 125, 1-8.
619 57. Li, W.; Liu, H. M.; Qin, G. Y., Structure characterization and antioxidant activity

620 of polysaccharides from Chinese quince seed meal. Food Chem. **2017**, 234, 314.
621 58. Lee, M. H.; Reich, D. H.; Stebe, K. J.; Leheny, R. L., Combined Passive and
622 Active Microrheology Study of Protein-Layer Formation at an Air−Water Interface.
623 Langmuir the Acs Journal of Surfaces & Colloids. **2010**, 26, 2650.
624 59. Tisserand, C.; Fleury, M.; Brunel, L.; Bru, P.; Meunier, G. In Passive
625 Microrheology for Measurement of the Concentrated Dispersions Stability, UK
626 Colloids 2011 - International Colloid and Surface Science Symposium, **2012**; pp
627 101-105.
628 60. Luo, D.; Li, Y.; Xu, B.; Ren, G.; Li, P.; Li, X.; Han, S.; Liu, J., Effects of inulin
629 with different degree of polymerization on gelatinization and retrogradation of wheat
630 starch. Food Chem. **2017**, 229, 35-43.
631 61. Lopes, S. M.; Krausová, G.; Rada, V.; Gonçalves, J. E.; Gonçalves, R. A.; de
632 Oliveira, A. J., Isolation and characterization of inulin with a high degree of
633 polymerization from roots of Stevia rebaudiana (Bert.) Bertoni. Carbohydr. Res. **2015**,
634 411, 15-21.
635 62. Critter, S. A. M.; Airoldi, C., Thermal analysis of brazilian tropical soils
636 originating from different sources. J.braz.chem.soc. **2006**, 17, 1250-1258.
637 63. Zha, X. Q.; Lu, C. Q.; Cui, S. H.; Pan, L. H.; Zhang, H. L.; Wang, J. H.; Luo, J. P.,
638 Structural identification and immunostimulating activity of a Laminaria japonica
639 polysaccharide. Int. J. Biol. Macromol. **2015**, 78, 429-438.

Table 1. Compositional, molecular and structural features of WGP isolated from wheat germ[a]

Polysaccharide	WGP
Mn/10^4 Da	460
Mw/10^4 Da	489
P_d	1.06
Protein (%)	5.57±0.98
Neutral sugar (%)[b]	81.45±0.24
Total pentosan (%)[b]	60.27±1.10
Uronic (%)	n.d.
L-arabinose	29.3
D-xylose	42.7
D-galactose	14.7
D-glucose	13.3
Arabinose/xylose	0.69
Yield (%)	0.075

n.d., not determined; [a] Data are presented as the mean (n=3); [b] Expressed as % of sample dry matter.

Table 2. GC-MS Data for the Methylated Sugar Moieties of WGP

Retention time(min)	Mass fragment(e/m)	Linkage	MethyIated sugar	Molar ratio(%)
A 19.489	42.8;44.8;87;99.0;233	1→3,6-Galp	2,4-Me_2-Galp	12.11
B 21.077	44.8; 87;101.1;129.1;160.9	terminal Glcp	2,3,4,6-Me_4-Glcp	14.52
C 21.483	71;99;101;188.9	1→5-Araf	2,3-Me_2-Araf	28.09
D 24.667	44.8;87;101.1;129.1;160.1	1→4-Xylp	2,3,-Me_2-Xylp	19.01
E 27.082	42.8;44.8;87;99;233	1→3,4-Xylp	2-Me-Xylp	26.27

Table 3. Assignment of 13C NMR and 1H NMR Chemical Shifts of WGP

Sugar residue		Chemical shifts(ppm)					
		C1/H1	C2/H2	C3/H3	C4/H4	C5/H5	C6/H6
A	→3,6)-β-D-Gal(1→	101.44/ 4.40	75.44/ 3.32	77.48/ 4.05	76.59/ 3.54	70.52/ 3.98	61.45/ 3.57
B	β-Glcp-(1 →	103.18/ 4.50	73.40/ 3.69	74.29/ 4.09	73.72/ 3.57	76.56/ 4.01	62.93/ 3.62
C	→5)-*α*-L-Ara(1→	109.21/ 5.24	84.70/ 4.24	83.87/ 3.63	82.40/ 4.00	61.20/ 4.39	
D	→4)-β-D-Xyl(1→	104.78/ 4.52	72.50/ 3.54	76.59/ 4.18	73.97/ 3.72	62.10/ 4.13	
E	→3,4)-β-D-Xyl(1→	107.37/ 5.09	77.48/ 4.10	84.13/ 3.71	83.40/ 4.24	61.78/ 3.83	

Table 4. The results of physicochemical properties of WGP.[a]

Sample	Concentration (mg/mL)	*TSI*	*MVI*×10^5	*EI*×10^{-4}	*SLB*
	0.1	0.45±0.18c	5.78±0.56a	6.25±0.12b	0.23±0.02e
	0.5	1.56±0.90c	2.03±0.14c	4.47±0.11d	0.46±0.04c
WGP	1	4.73±1.98c	1.98±0.16c	4.50±0.10d	0.47±0.05b
	3	18.73±8.90b	4.63±0.36b	7.53±0.086a	0.33±0.03d
	5	23.15±10.87a	0.37±0.00d	5.27±0.063c	0.88±0.01a

aData are expressed as means ± SD, n = 3, Different letters (a, b, c, d,e) in the same column represent significant differences between different treatments ($p < 0.05$).

Table 5. Thermal parameters from TGA and DSC measurements-weight loss at 800 ^{o}C, degradation temperature (Td), denaturation peak temperature (Tp), onset temperature (To), endset temperature (Te) and enthalpy (ΔH) are given in parenthesis.

Sample	Weight loss (%)	Td(^{o}C)	To(^{o}C)	Tp(^{o}C)	Te(^{o}C)	ΔH(J/g)
WGP	88.42%	290.03	32.7	82.57	126.77	354.22

Figure captions

Figure 1. Chromatography of the polysaccharides from wheat germ by Sephacryl S-500 HR column (A) and Sepharose 4 B gel-permeation chromatography (B); UV spectrum (C) of WGP; HPLC profile (D) of WGP. (WGP: polysaccharide from wheat germ)

Figure 2. Structure analysis profiles. Gas chromatograph (A) of Smith degradation of WGP; FT-IR spectral (B) analysis of WGP; (C) Maximum absorption of WGP-Congo red complex in solution with various concertration of NaOH. (WGP: polysaccharide from wheat germ)

Figure 3. ^{1}D and ^{2}D NMR spectra of WGP (A) ^{1}H NMR spectrum; (B) ^{13}C NMR spectrum; (C)^{1}H-^{1}H COSY spectrum; (D)^{1}H-^{13}C HMQC spectrum; (E)^{1}H-^{13}C HMBC spectrum). (WGP: polysaccharide from wheat germ)

Figure 4. Predicted repeating unit of WGP (polysaccharide from wheat germ) from the wheat germ.

Figure 5. Scanning electron micrograph and atomic force microcopy images of WGP.(A)SEM (B)AFM(polysaccharide from wheat germ).

Figure 6. Effect of different concentration on the physical stability (*TSI*) of WGP (polysaccharide from wheat germ).

Figure 7. Thermal analysis profiles of WGP. (A)TG and DTG curve; (B) DSC curves.

Figure 8. Effects of WGP on cell viability(A) and production of Cytokine Secretion(TNF-α and IL-8) of RAW264.7 macrophages. Values are presented as means ± SD (n = 10); ∗ and ∗∗ represent $p < 0.05$ and $p < 0.01$ compared with control,

respectively.

Figures

Figure 1

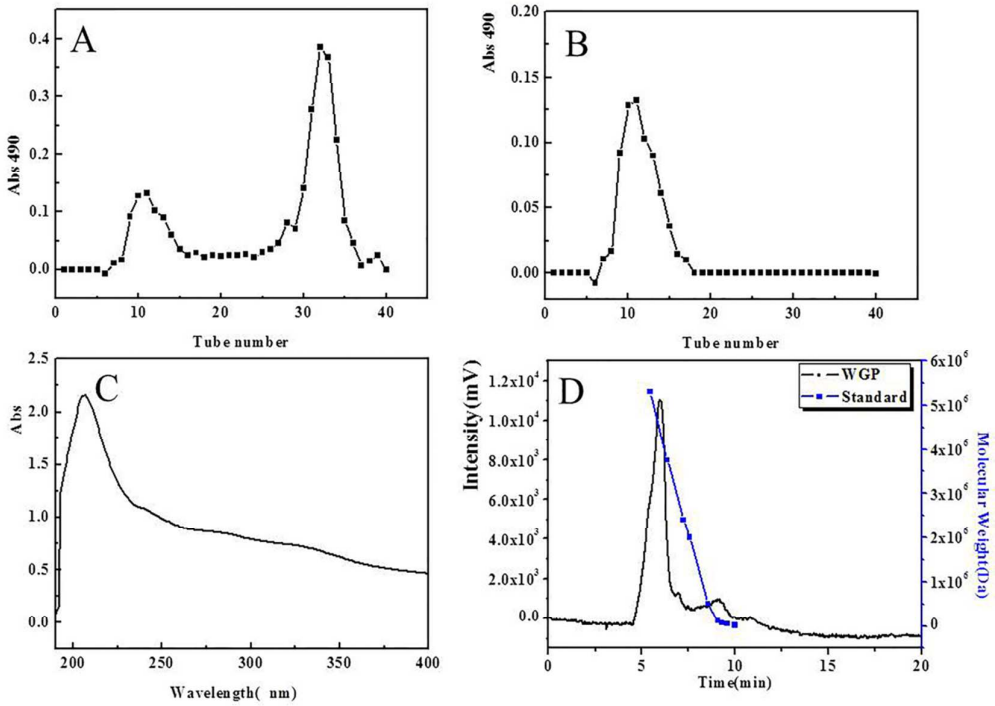

Figure 2

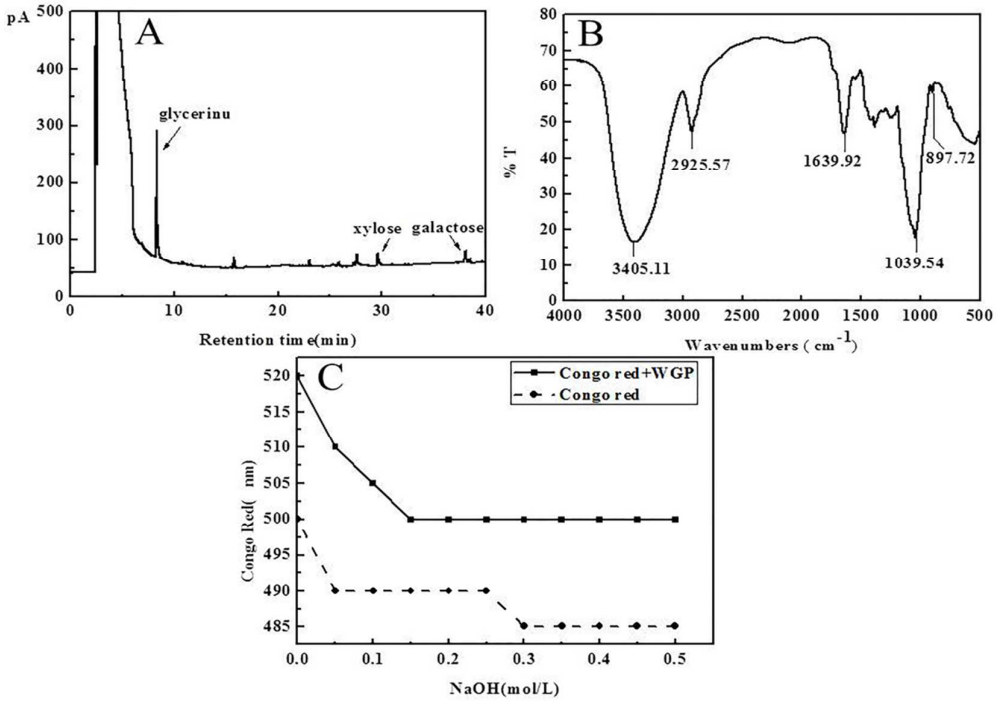
A
pA
glycerinu
xylose
galactose
Retention time(min)
B
% T
2925.57
1639.92
897.72
3405.11
1039.54
Wavenumbers (cm-1)
C
Congo red+WGP
Congo red
Congo Red(nm)
NaOH(mol/L)

Figure 3

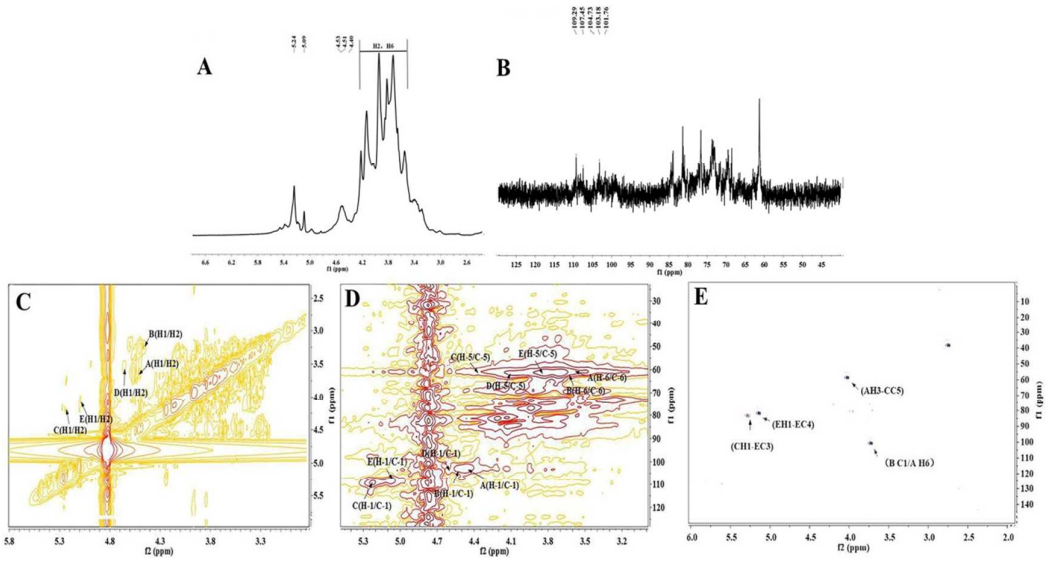
A
B
C
D
E
f1 (ppm)
f2 (ppm)
B(H1/H2)
A(H1/H2)
D(H1/H2)
E(H1/H2)
C(H1/H2)
C(H-5/C-5)
E(H-5/C-5)
A(H-6/C-6)
D(H-5/C-5)
B(H-6/C-6)
D(H-1/C-1)
E(H-1/C-1)
A(H-1/C-1)
B(H-1/C-1)
C(H-1/C-1)
(AH3-CC5)
(EH1-EC4)
(CH1-EC3)
(B C1/A H6)

Figure 4

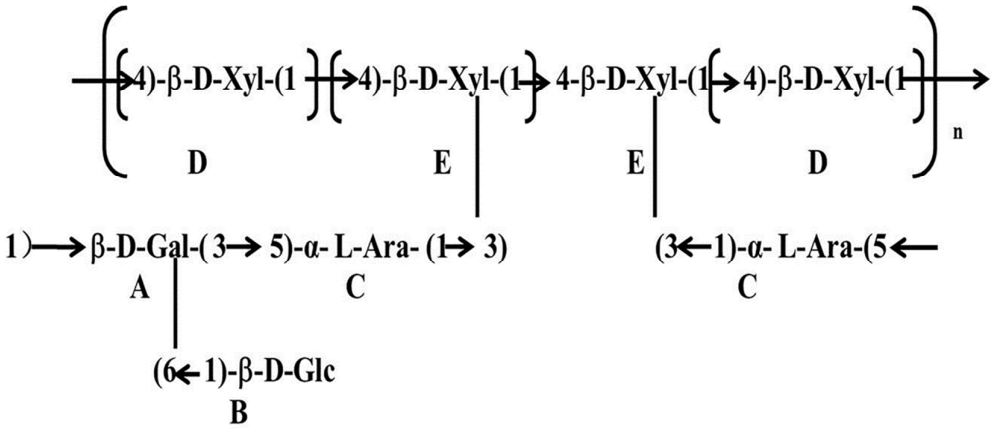
4)-β-D-Xyl-(1
4)-β-D-Xyl-(1
4-β-D-Xyl-(1
4)-β-D-Xyl-(1
n
D
E
E
D
1)
β-D-Gal-(3
5)-α- L-Ara- (1
3)
(3
1)-α- L-Ara-(5
A
C
C
(6
1)-β-D-Glc
B

Figure 5

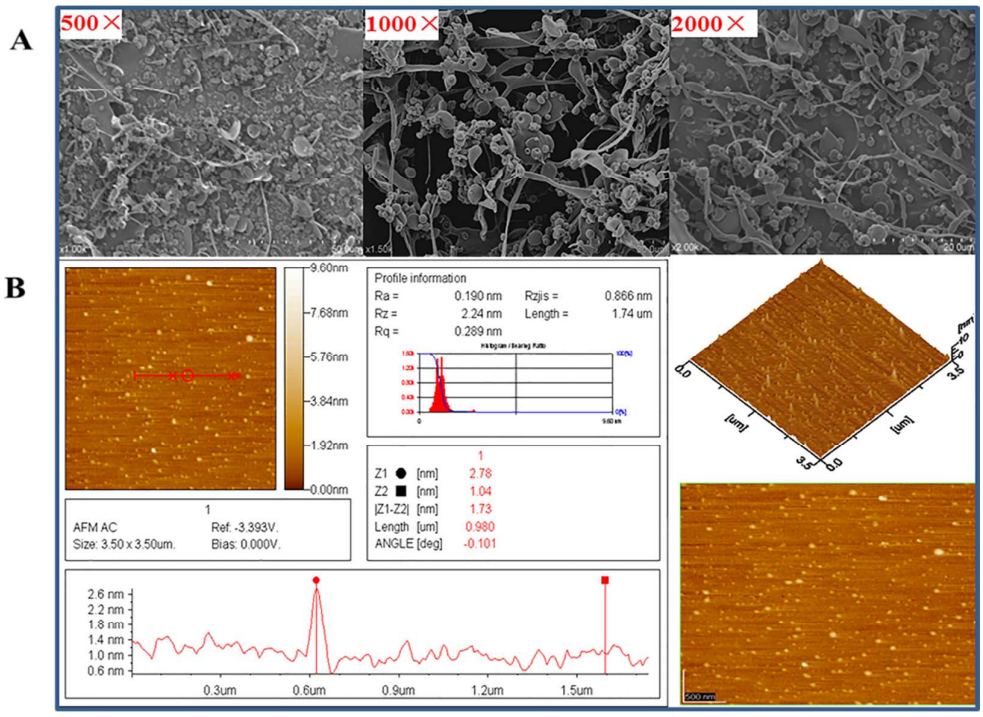
A
500×
1000×
2000×
B
9.60nm
7.68nm
5.76nm
3.84nm
1.92nm
0.00nm
Profile information
Ra = 0.190 nm
Rzjis = 0.866 nm
Rz = 2.24 nm
Length = 1.74 um
Rq = 0.289 nm
AFM AC
Ref. -3.393V.
Size: 3.50 x 3.50um.
Bias: 0.000V.
Z1 [nm] 2.78
Z2 [nm] 1.04
|Z1-Z2| [nm] 1.73
Length [um] 0.980
ANGLE [deg] -0.101
2.6 nm
2.2 nm
1.8 nm
1.4 nm
1.0 nm
0.6 nm
0.3um
0.6um
0.9um
1.2um
1.5um
[um]
[um]

Figure 6

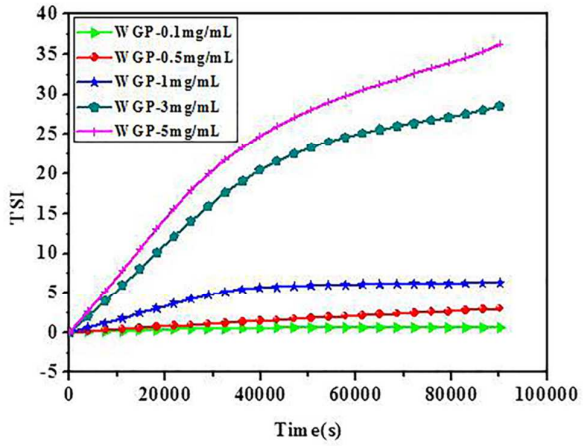
WGP-0.1mg/mL
WGP-0.5mg/mL
WGP-1mg/mL
WGP-3mg/mL
WGP-5mg/mL
TSI
Time(s)
40
35
30
25
20
15
10
5
0
-5
0
20000
40000
60000
80000
100000

Figure 7

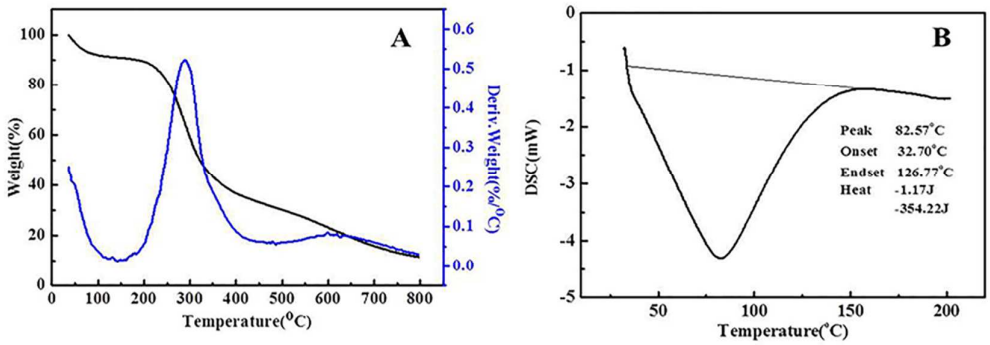
A
Weight(%)
Deriv.Weight(%/°C)
Temperature(°C)
B
DSC(mW)
Temperature(°C)
Peak 82.57°C
Onset 32.70°C
Endset 126.77°C
Heat -1.17J
-354.22J

Figure 8

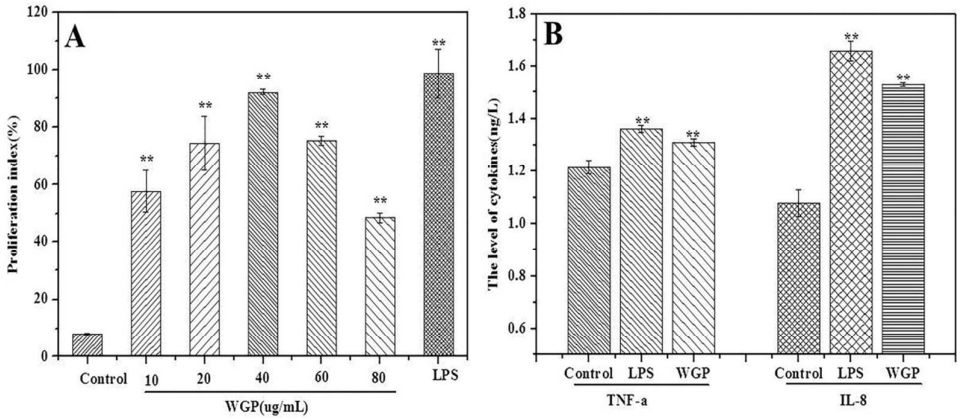
A
Proliferation index(%)
120
100
80
60
40
20
0
Control
10
20
40
60
80
LPS
WGP(ug/mL)
B
The level of cytokines(ng/L)
1.8
1.6
1.4
1.2
1.0
0.8
0.6
Control
LPS
WGP
TNF-a
Control
LPS
WGP
IL-8

TABLE OF CONTENTS GRAPHICS